Shock Wave Diffraction at the Inclined Exit of a Shock Tube

R.T. Paton and B.W. Skews

1 Introduction

While many studies have been made of the diffraction of a shock wave from the end of a conventional cylindrical shock tube (for example; [3, 2, 6]), or from shock tubes with non-axisymmetric cross-sections or exits (for example; [1, 4, 7]), very little has been done experimentally on the diffraction of a shock wave around the exit of a shock tube inclined to the axis of the flow. A study undertaken by Kim et al. [5] explored this field but focused primarily on computational modelling of the flow, with the simplifying treatment of the field as two-dimensional. The experimental images were also not very clear.

The current work presents the results of an experimental study using a conventional diaphragm-constrained, air-driven, circular cross-section shock tube expanding into ambient conditions producing shock Mach numbers between 1.25 and 1.64. The end of the shock tube was modified by the attachment of various sections cut off at angles to the normal ranging from 30° to 60°. The attached exhaust sections also included a plate attached in the plane of the exit, approximately 400*mm* square, to remove the characteristic length of the pipe thickness by preventing diffraction of the shock wave over the shock tube exterior.

2 Results

Fig. 1 shows the development of the flow field for Mach numbers of 1.28, 1.46, and 1.64 and an inclination of the end of the shock tube to the normal of 30°. Key frames have been selected to illustrate the development of the flow field.

R.T. Paton · B.W. Skews
Flow Research Unit, School of Mechanical, Industrial & Aeronautical Engineering,
University of the Witwatersrand, 1 Jan Smuts Avenue, Johannesburg,
WITS 2050, South Africa

R. Bonazza and D. Ranjan (eds.), *29th International Symposium on Shock Waves 2*,
DOI: 10.1007/978-3-319-16838-8_78

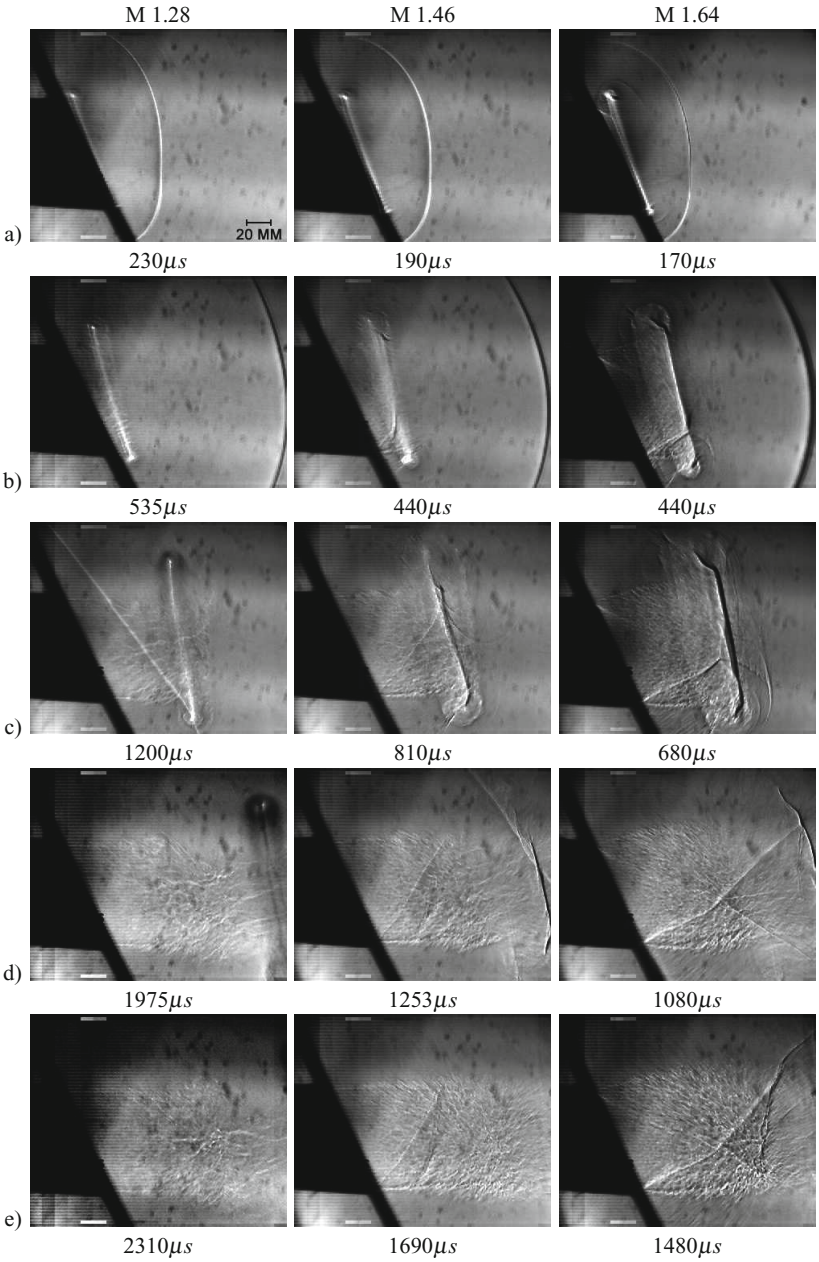

Fig. 1 The development of the flow field for shock diffraction from the exit of a shock tube inclined 30° to the normal for Mach numbers of 1.248, 1.46, and 1.64. Approximate time since the arrival of the incident wave at the upstream diffracting edge is given

The selected flow field stages are: when the diffracted shock wave first exits the frame; when the shock wave reaches approximately 2 tube diameters downstream; when the vortex ring formed at the exit of the shock tube has convected approximately 1 tube diameter (4") away from the exit plane; when the vortex ring is approximately 2 tube diameters downstream; and when the vortex ring (not shown) is approximately 3 tube diameters downstream.

2.1 The General Nature of the Diffraction

A primary difference between the canonical diffraction at the normal exit of a shock tube and the cases studied here is that the diffraction of the shock wave is not simultaneous at all azimuths. The end result of this is that the vortex shed at various azimuthal positions, if any, varies in 'age' and strength with points farther upstream being more developed than those downstream. Also, the angle of diffraction changes from a very oblique one upstream to an acute one downstream and thus the strength of the expansion wave formed varies, especially after the horizontal centreline position where the diffraction angle reaches 90° and the subsequent acute diffractions decrease in strength (while diffractions greater than 90° are basically independent of angle).

The final feature of this change in diffraction behaviour is that the time taken for total diffraction (i.e. he time taken for the incident shock wave to travel along the length of the exit from its most upstream to most downstream edge) ranges from approximately 100 μs to 370 μs depending on exit angle and Mach number. The result of this is that for higher exit angles and lower Mach numbers, the shock wave diffracting at the downstream edge of the exit is often no longer plane and uniform in strength as it has been affected by the expansion waves originating at other parts of the diffracting edge.

2.2 Initial Diffraction

In Fig. 1 frames a), it can be seen that the vortex produced by the initial diffraction of the shock wave appears thicker at the upstream edge than at the downstream edge. The contrast within the vortices also increases with Mach number suggesting greater density gradient within the vortices and therefore higher velocity gradients. The stand-off distance of the upstream part of the vortex from the diffracting edge also increases with Mach number, confirming the greater induced velocity of this section and hence the greater velocity within that portion of the vortex. In the first frame for Mach 1.64 the interaction of the expansion waves produced at the edges on the centreline axis can just be seen to be interacting. There is also a possible shocklet in the outer portion of the top section of the vortex.

2.3 Convection of the Vortex

Frames b) of Fig. 1 show the position of the vortex when the axial portion of the shock wave is just at the limit of the field of view. It is clearly noticeable that the convection speed of the vortex increases significantly with Mach number, with the vortex produced by the Mach 1.64 incident wave having travelled approximately 4 times the distance of that produced by the Mach 1.28 wave. An induced shock wave in the surface passing through the centreline of the vortex loop is visible in the Mach 1.64 case, and there is a shock wave inclined to this surface and apparently associated with the downstream diffracting edge in the Mach 1.46 case. Notably, this shows a delay in the formation of the induced shock wave in the Mach 1.46 case, even though it is above the Mach 1.42 limit identified in [2] for the formation of an embedded shock wave for the plane vortex ring. A bend in the induced shock wave at the intersection of the vortex loop and vertical centre plane is also noticeable, though this is actually a shocklet induced in the outer portion of the vortex as seen at earlier times.

2.4 Evolution of Vortex Structures and the Jet

Fig. 1 frames c show the flow fields for the different Mach numbers when the vortex has convected one tube diameter downstream. The induced shock wave is now fully formed in the Mach 1.46 case, though it is noticeable that it appears to have two fronts in the upper portion. This is due to the interaction of the remnants of the shock wave seen at earlier times with the main induced shock wave. The earlier wave weakens considerably as time progresses and this interaction changes to that with the weak shock wave seen to originate at the downstream diffracting edge. It is believed that this shock wave forms to correct a pressure imbalance due to the varying strength of the diffraction around the periphery of the exit, although the evident bulge in the jet boundary suggest that it is underexpanded (as would be expected). The rough shape of the weak shock suggests that it doesn't occur in the centre plane but rather that it is formed away from the centre plane and interacts with the turbulent jet boundary. Additional visualisation of this feature from other azimuth positions will be needed to confirm its shape.

It is also notable that a similar weak shock wave appears to form from the upstream diffracting edge for the Mach 1.64 case. The jet boundary here is also significantly inclined away from the axis of the system largely due to the induced flow from the significantly stronger vortex and its convection away from the axis at early times.

Finally, a weak shock wave can be seen in the Mach 1.28 case. This wave appears to originate significantly far upstream on the shock tube, although it does seem to interact with the centreline flow (as seen by the change in shape where it meets the downstream portion of the vortex). This wave is evident for all Mach numbers and does change in strength with changes in incident wave strength. Although it

was originally attributed to recoil of the shock tube (since it is entirely supported on casters), this hypothesis has not been confirmed. Another possible source of this wave is the reflection of the incident shock wave off elements of the flow visualisation system, which would explain the dependence of the wave strength on incident wave strength, though this must also be tested in more detail. In all cases, it seems that this wave is significantly weaker than the incident wave and appears to have a negligible effect on the vortex and associated flow field.

2.5 Late Time Jet Flow

In frames d) of Fig. 1, the vortex is just leaving the visible flow field. At Mach 1.28 the jet appears aligned with the tube axis and is fairly uniform, although there is noticeable turbulence in the jet boundary. At Mach 1.46, the weak shock wave evidently associated with the downstream diffracting edge has persisted though it appears to terminate in the jet boundary. At Mach 1.64 there is a reflection of the weak shock wave structures with an associated shear layer from the interaction point(s). The jet also appears significantly inclined upward.

At later times the Mach 1.28 jet appears unchanged while another shock wave interacting with the jet boundary has formed in the Mach 1.46 jet. The wavering position of this shock and its rough shape again suggest interaction with the turbulent jet boundary and the extent of the shock across the jet cross-section cannot be surmised from these images. In the Mach 1.64 case, a downstream shock wave is also evident in the jet boundary, but here it has terminated the reflected shock waves formed earlier. This suggests that the weak shock waves in the jets are approximately conical in shape and the precise geometry of the reflection will need further exploration.

Another feature noted in the Mach 1.67 flow field is the disruption of the shear layer produced at the weak shock wave reflection by the induced shock wave, and the subsequent entrainment of the disrupted shear layers into the vortex periphery. A sample of this is shown in Fig. 2 a).

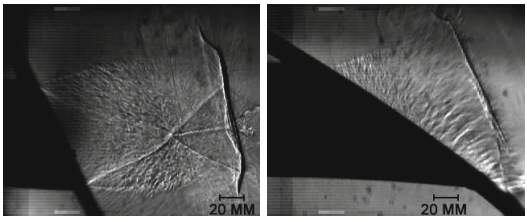

Fig. 2 a) Detail of 30°, Mach 1.64 flow field (t = 960 μs) showing disruption of the shear layer through the induced shock wave, and b) an example of the flow field induced by the diffraction of a Mach 1.64 shock wave from a 60° inclined shock tube exit (t $\approx$ 830 μs)

3 Variation of Flow Field with Angle

As can be seen in Fig. 2 b), the flow field produced by the diffraction from a shock tube exit of higher inclination to the normal is qualitatively similar to that produced at lower angles, though there are several distinctions. First, the inclination of the jet to the axis of the tube is marked, though it appears to be more a broadening of the jet away from the axis in the region produced by the diffraction of the shock wave over the upstream diffracting edge. Also, the induced shock wave does not appear to extend entirely to the lower vortex core shed from the downstream diffracting edge. This would be because the vortex shed here is significantly weaker because the shock wave diffracted only through an angle of 30° on the centre line and thus the local induced velocity is too low for the shock wave to form. The induced shock wave must, therefore, terminate in the space inside the vortex ring and is expected to be of a crescent shape when viewed along the axis.

4 Conclusion

The diffraction of a shock wave from the exit of a shock tube at even modest inclination to the normal produces a complex flow field with structures not seen in the canonical diffraction. Increasing the angle of inclination will likely exaggerate these differences and this will be explored further in coming work. Although CFD could provide valuable insight into the structure of the complex flow field formed, work to date has proved incapable of capturing all of these features and more refinement of these models will be needed before this approach might prove useful.

References

1. Abe, A., Watanabe, M.: Three dimensional flow structure behind a shock wave discharged from a rectangular cross section shock tube. In: Takayama, K. (ed.) Shock Waves: Proceedings of the 18th International Symposium, Sendai, Japan, July 21-26, pp. 209–212. Springer (1991)
2. Brouillette, M., Hébert, C.: Propagation and interaction of shock-generated vortices. Fluid Dyn. Res. 21(3), 159–169 (1997)
3. Elder, F.K., De Haas, N.: Experimental study of the formation of a vortex ring at the open end of a cylindrical shock tube. J. Appl. Phys. 23(10), 1065–1069 (1952)
4. Jiang, Z., Onodera, O., Takayama, K.: Evolution of shock waves and the primary vortex loop discharged from a square cross-sectional tube. Shock Waves 9(1), 1–10 (1999)
5. Kim, H.-D., Kweon, Y.-H., Setoguchi, T.: A study of the impulsive wave discharged from the inclined exit of a tube. P I Mech. Eng. C-J Mec. 217, 271–279 (2003)
6. Kleine, H., Vo Le, C., Takehara, K., Etoh, T.G.: Time-resolved visualization of shock-vortex systems emitted from an open shock tube. J. Visual-Japan 13(1), 33–40 (2009)
7. Zare-Behtash, H., Kontis, K., Gongora-Orozco, N., Takayama, K.: Shock wave-induced vortex loops emanating from nozzles with singular corners. Exp. Fluids 49(5), 1005–1019 (2010)